Bioactive Materials 5 (2020) 510–515

Contents lists available at ScienceDirect

Bioactive Materials

journal homepage: http://www.keaipublishing.com/biomat

Improving mechanical and antibacterial properties of PMMA via polyblend electrospinning with silk fibroin and polyethyleneimine towards dental applications

Ugur Yunus Karatepe, Tugba Ozdemir*

Molecular Biology and Genetics Department, Tokat Gaziosmanpasa University, Tasliciftlik, Tokat, Turkey

ARTICLE INFO

Keywords:
Dental biomaterials
Reinforced
Bacterial resistance
PEI
SF

ABSTRACT

Poly(methylmethacrylate) (PMMA) is a widely used material in dental applications, particularly as denture resins. Due to thermally unstable and wet oral cavity, the implanted PMMA based resins occasionally deform and grow bacterial biofilms at the interface between oral cavity and the biomaterial. Several strategies attempted earlier to improve the bacterial resistance and mechanical performance of PMMA. Poly(ethyleneimine) (PEI) is a hyperbranched cationic polymer shown earlier to improve antibacterial activity of resins but do not improve mechanical properties of the resins alone, while silk fibroin (SF) is a natural biopolymer with unique material properties. In this study, we combined SF and PEI towards development of antibacterial and mechanically superior PMMA based materials towards overcoming its drawbacks. Using polyblend electrospinning to combine SF, PEI and PMMA, we successfully developed intrinsically antibacterial and mechanically reinforced nanofiber mats. We propose that the resulting nanofiber mats have the potential to be incorporated into PMMA based denture resin materials to overcome the problems of patients and improve their quality of life.

1. Introduction

Increasing the quality of life among aging population has become an emerging topic due to the difficulties aged individuals suffer on a day-to-day basis. One of the most common problems in the aging population is bone loss and accompanying loss of teeth. Denture based resins has been the outstanding solution to this problem since as early as the first applications of dentistry [1]. Most of the denture resins are composed of polymeric materials and Poly(methylmethacrylate) (PMMA) has been the material of choice due to its superior mechanical properties and aesthetic appeal [2].

PMMA is the gold standard biomaterial in several biomedical applications and used since mid 1930s [3]. The polymerization of PMMA often achieved via free radical polymerization, however other anionic and coordination polymerization routes are also possible. PMMA is a thermoplastic polymer having a glass transition temperature (T_g) of 130 °C and due to its amorphous structure, it is easily processed into desired shapes and because PMMA is clear, it is useful in optics but also applications that require aesthetic appeal. However, PMMA has several disadvantages due to its propensity for fatigue failure [4], inferior bending and fracture resistance and thermal instability and susceptibility for bacterial growth. Improving disadvantages associated with PMMA in denture applications will relieve the burden users experiencing and may extend the lifetime of dentures and improve patient's quality of life. Several strategies have developed to increase the performance of PMMA such as utilizing copolymers with PMMA, incorporating fillers or fibers inside the PMMA resins or curing in different conditions [5–7]. Embedded fibers often added to improve flexural properties of PMMA resins while metal, polymer or mineral particles are added to supply strength and often times bacterial resistance to PMMA [8].

Antibacterial additives into PMMA based denture resins have employed earlier [9]. Al_2O_3 and TiO_2 nanoparticles are successful approaches used in the past to overcome bacterial film formation however their cytotoxicity pose great risk for their use in denture resins. Using polymers as denture additive is another strategy to overcome biofilm formation. For instance, hyperbranched highly cationic polymers such as Poly(ethyleneimine) (PEI) interacts with the polar acid groups on the bacterial cell wall and leads to ultimate destruction of cell membrane and has been successfully used as a denture additive in the form of nanoparticles earlier [10]. However, addition of PEI particles more than 1% w/v result loss fracture resistance and mechanical properties of the

Peer review under responsibility of KeAi Communications Co., Ltd.
* Corresponding author. Molecular Biology and Genetics Department, Tokat Gaziosmanpasa University, Tokat, Turkey.
E-mail address: tugbaozdemir.tr@gmail.com (T. Ozdemir).

https://doi.org/10.1016/j.bioactmat.2020.04.005
Received 10 January 2020; Received in revised form 2 April 2020; Accepted 5 April 2020

resins [11]. Therefore it is important to develop a strategy to introduce PEI without loss of resin's mechanical strength.

Silk is one of the most versatile fibrillar structure in nature that is produced by *Bombyx mori* silkworms and spiders [12]. The superior elastic strength that lies in silk fibrils rise from silk fibroin (SF) protein. SF comprise the core of the core-sheath structure of silk fibrils. SF is a protein containing semi-crystalline regions that has repeating Gly-Ser-Gly-Ala-Gly-Ala peptide motifs and connected with amorphous units. The strong semi-crystalline beta-sheet structures (65% of the whole protein) are bound together with flexible amorphous regions (35%) forms the unique protein structure of SF [13]. SF has been utilized as a safe, biocompatible and strong biomaterial in several tissue engineering applications [14]. When combined with other polymers, SF shown to enhance mechanical and flexural properties [15]. However, processing SF using organic solvents that has been used in polymer processing greatly diminishes its protein ultrastructure thus limiting its applicability in industrial production.

Electrospinning is a material fabrication method to develop fibers with desired properties [16]. By extruding a polymer solution using a high voltage source, fibers with varying physical and mechanical properties can be developed [17]. Polyblend electrospinning is a technique to combine polymers with different properties into one reservoir and electrospin together to form fiber mats containing collective properties of individual polymers otherwise cannot be combined [18]. During polyblend electrospinning different polymer chains entangle with one another to form nanofibers and it is important to consider miscibility and charge-charge interactions of polymers being cospun in order to better control desired fibril morphology. For instance, during polyblend electrospinning, positively charged polymer side groups could interact with negatively charged groups in the neighboring polymer could lead to electrostatic interactions and therefore alter intrinsic material properties such as elastic modulus, hydrophobicity or polymer melting temperatures [16].

In this study, we devised a novel strategy to build PMMA based polyblend fibers with increased mechanical and thermal properties with added antibacterial activity to one of the main oral pathogen *p. aeruginosa.* Through polyblend electrospininning PMMA with SF and PEI, we created nanofiber mats with smaller fibril diameter and high melting temperatures leading to reinforcement of PMMA alone. The resulting polymer nanofiber mats comprised mainly of PMMA, can serve as a potential antibacterial additive to PMMA based denture resin applications and thus overcome problems denture patients experiencing.

2. Materials and methods

2.1. Materials

PMMA (Mw = 360,000 Da), hyperbranched PEI (Mw = 25,000 Da), lithium bromide (LiBr), sodium bicarbonate ($NaHCO_3$), Spectra/Por brand dialysis membrane with a 10,000 kDa molecular weight cutoff (MWC), LB Broth Agar powder were purchased from Sigma-Aldrich (St Louis, MO, USA), dimethylformamide (DMF), Analytical grade Acetone were from Fisher Scientific (New Hampton, NH, USA). Cocoons from *bombyx mori* silkworms were purchased from Kozabirlik (Bursa, Turkey).

2.2. Preparation of SF from bombyx mori cocoons

Cocoons from *Bombyx mori* silkworms were first minced into small pieces and cleaned from any residues from dead silkworms. The minced pieces were boiled in a 0.02 M $NaCO_3$ solution for 60 min until Sericin and Fibroin is dissociated from each other and a relaxed fibroin yarn was obtained. The SF yarn then washed with ultrapure water thrice for 10 min each. The washed SF yarn moved into a fume hood and dried overnight. The next day, dried SF weighed and 4 g of SF yarn was dissolved in 40 ml of 9.3 M LiBr solution at 60 °C for 2 h. After the SF dissolution is confirmed, the SF solution transferred into a 10 kDa MWC dialysis membrane and dialyzed against ultrapure water and changed at 1, 4, 24 and 48 h time points. Following dialysis, the protein concentration was measured by using its absorbance at 280 nm(Molar extinction $Coefficient_{SF}$ = 473,480 M^{-1} cm^{-1}). We created SF microparticles following earlier methods [19] before homogenizing in electrospinning solvent to protect SF ultrastructure. Formation of SF microparticles were confirmed by a particle size analyzer as shown in Fig. S1. (Malvern-MS2000, Malvern, UK). The SF solution concentration was adjusted to 10 mg/ml using ultrapure water and acetone was added while being homogenized at 10,000 rpm. The resulting SF microparticles were further allowed to fully dry before further experiments.

Table 1
Polymer (PMMA, PEI) and Protein (SF) weight/volume (w/vol) ratios in electrospinning solutions.

	PMMA	PMMA + SF	PMMA + PEI	PMMA + SF + PEI
Polymer content (w/vol)	8%	7% PMMA 1% SF	7% PMMA 1% PEI	6% PMMA 1% PEI 1% SF

2.3. Electrospinning

Four different protein-polymer mixtures were electrospun for the study as shown in Table 1 all of which homogenized in DMF as the carrier solvent for electrospinning. The polymer or protein-polymer solvents were allowed to dissolve by constant agitation at room temperature overnight. The solvents then transferred to a 5 ml syringe with a 21 G blunt tip needle. Syringe was loaded onto a syringe pump (New Era Pump systems, NE-300, Farmingdale, NY, USA) and extrusion rate adjusted to 1.4 ml/h. The syringe tip to collector distance was set to 20 cm and 20 kV voltage was applied between the needle tip to a aluminum foil covered collector for 8 h. The resulting fiber mats were collected and stored at room temperature before testing.

2.4. SEM imaging

Fiber morphology and diameter was assessed using scanning electron microscopy (SEM). A field emission SEM (TESCAN, MIRA3, Brono, Checzk Republic) was used to image the fibers after sputter coating with thin layer of gold deposited for 3 min at a 20 mA current. The obtained images were used for diameter quantification at NIH ImageJ (Bethesda, MD, USA) software.

2.5. Fourier transform infrared (FTIR) analysis

The chemical properties of the resultant matrices was first assessed with FTIR spectroscopy using Jasco 2000 Spectra (Tokyo, Japan). Using ATR function, the fiber chemical bond vibrations were characterized using infrared light and tabulated using the Spectra Viewer software.

2.6. Differential scanning calorimetry (DSC) analysis

Changes in thermal behavior and melting temperatures of resulting fiber mats were analyzed using NETZSCH DSC 214 Polyma (Boston, MA, USA). Briefly 5 mg of fiber mat was weighed and placed in aluminum DSC chambers and heated from −30 °C to 180 °C at a 10 °C/min speed under nitrogen gas flow of 60 ml/min.

2.7. Tensile testing

Mechanical properties and elastic modulus of the fiber mats were characterized using universal material testing device Instron 3345

(Norwood, MA, USA) at Kayseri Erciyes University School of Dental Medicine Central Laboratories. The fiber mats were cut into dog-bone shape samples (2.75 mm wide and 7.5 mm length) following the protocol described earlier [20]. Samples (n = 5) were loaded into the clamps of the testing machine and extended using a 50 N load cell at a 10 mm/min extension rate until the material failed. The stress-strain values were used to calculate elastic modulus of each sample. Average thickness of each mat was recorded as 0.18 ± 0.007 mm for PMMA, 0.32 ± 0.06 mm for PMMA + PEI, 0.19 ± 0.03 mm for PMMA + SF and 0.21 ± 0.01 mm for PMMA + SF + PEI.

2.8. Agar diffusion testing

Bacterial growth solid surfaces were prepared using nutrient agar and agar bacteriologique (Sigma Aldrich, St Louis, MO, USA). Briefly, nutrient agar solution mixture were autoclaved at 121 °C for 15 min and transferred into 10 mm petri dishes when the temperature reached to 45 °C. Allowed to solidify in an oven set to 37 °C overnight. The next day the bacterial suspensions adjusted to 0.4 OD_{600} seeded onto the agar plate then spreaded evenly onto the culture surface. Following bacterial inoculation, the disc shape (D = 6 mm) sample were placed onto the quadrant of the agar plate (n = 3 agar plate) and cultured 24 h before visual assessment of antibacterial zone formation. *P. Aeruginosa* bacterial strain was a gift from Prof. Dr. Isa Gokce from Tokat Gaziosmanpasa University.

2.9. Statistical analysis

All data in the study is presented as mean ± standard deviation (SD). Statistical analysis performed using two-sample *t*-test when comparing two group, one-way ANOVA was performed when comparing multiple groups.

3. Results

3.1. Morphology of fibers

We kept needle to collector distance, voltage, polymer extrusion rate, final material percentage (8% w/v) and electrospinning solvent the same across all experimental groups as seen in Table 1. Morphology of post-electrospun PMMA, PMMA + SF, PMMA + PEI and PMMA + SF + PEI fiber mats was shown in Fig. 1A and B, C and D respectively. The observed differences in fiber morphology in the SEM images show the PMMA + SF + PEI fibrils were relatively thinner compared to other experimental groups. Then we quantified the fibril diameters. Fig. 1. E show the average fibril diameter in each fiber mat.

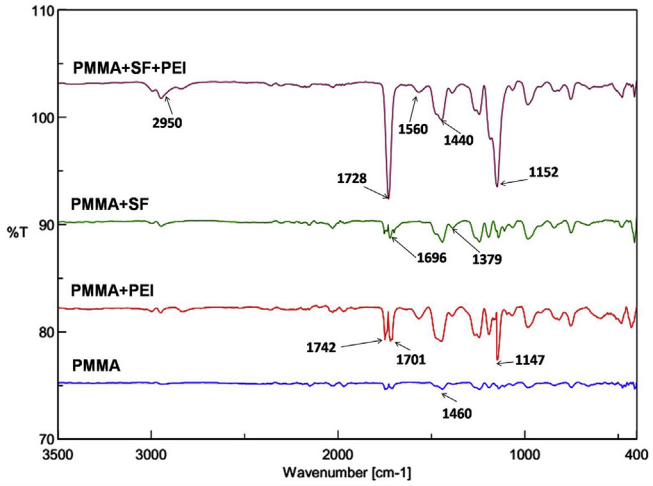

Fig. 2. FTIR Spectra of PMMA, PMMA + PEI, PMMA + SF and PMMA + SF + PEI nanofiber mats.

In accordance with the SEM images, the average fiber diameter in PMMA + SF + PEI mats were smaller than PMMA only, PMMA + SF or PMMA + PEI fibers. The measured fiber diameters for PMMA fibers were 0.52 ± 0.107 μm, PMMA + SF fibers 0.51 ± 0.117 μm, PMMA + PEI fibers 0.62 ± 0.212 μm and PMMA + SF + PEI fibers 0.25 ± 0.0502 μm. Compared to PMMA only fibers, PMMA + SF + PEI fibers resulted in 51.92% decrease in fibril diameter.

3.2. Fourier transform infrared (FTIR) spectroscopy analysis of fiber mats

Attenuated total reflectance (ATR)-FTIR was performed to investigate molecular footprint of each fiber mat. FTIR spectra of PMMA mats was used to serve as a reference to compare interactions of each additive on the overall chemical information of the resulting fibers (Fig. 2). PMMA nanofiber mats show CH_3 vibrations in addition to characteristic ester bonds between 1000 cm^{-1} to 1300 cm^{-1} [21]. The PMMA + PEI nanofibers show carbonyl stretch at 1742 cm^{-1} respectively and NH bending vibration at 1147 cm^{-1} [22]. From the characteristic vibration bands in pristine SF, only Amide I (C═O stretching) at 1696 cm^{-1} and Amide III (C–N stretching) at 1379 cm^{-1} is present in PMMA + SF nanofiber mats [23]. Combination of highly anoinic PEI and cationic SF together in the presence of PMMA resulted in the formation of C═O stretch at 1728 cm^{-1} in addition to N–H bending at

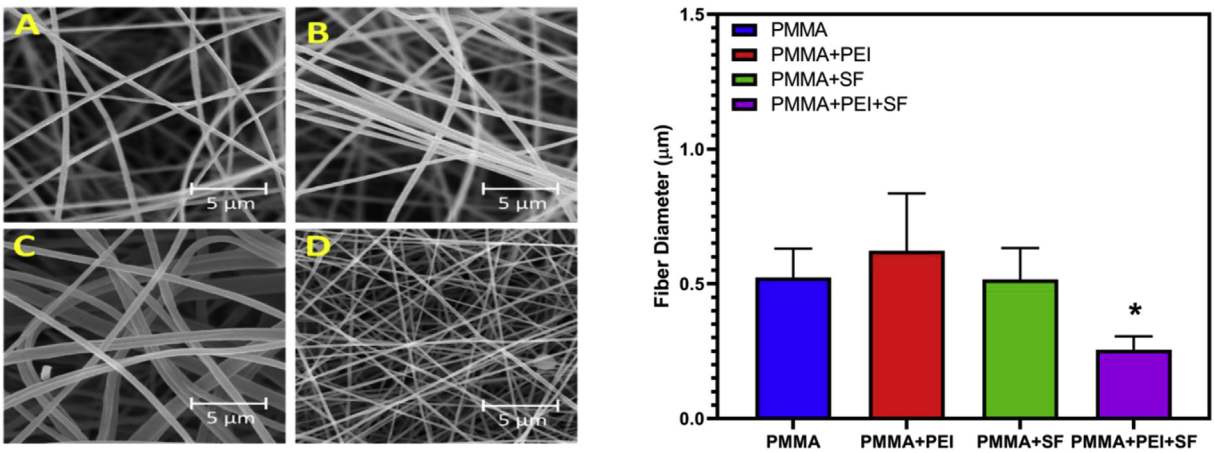

Fig. 1. SEM images of PMMA (A), PMMA + SF (B), PMMA + PEI (C) ve PMMA + SF + PEI (D) electrospun fibers. Average fiber diameter measurements (n = 100 fibers from 4 different images) from SEM images (* represents $p < 0.001$ compared to PMMA, PMMA + SF and PMMA + PEI).

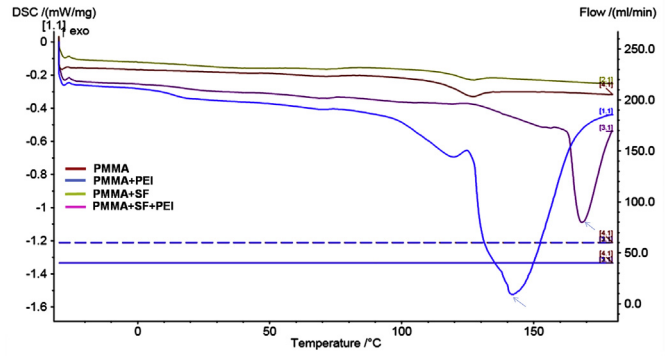

Fig. 3. Melting curves of PMMA (red), PMMA + PEI (blue), PMMA + SF (yellow) and PMMA + SF + PEI (pink) fiber mats. (For interpretation of the references to colour in this figure legend, the reader is referred to the Web version of this article.)

1560 cm^{-1} and CH stretching at 1440 cm^{-1}. The asymmetric C–N bending apeear at 1152 cm^{-1} [21]. C–H stretching vibrations at methyl groups at 2950 cm^{-1} also appeared to have higher signal at PMMA + SF + PEI fibers.

3.3. Thermal analysis of fiber mats

DSC thermograms of PMMA, PMMA + PEI, PMMA + SF and PMMA + SF + PEI fiber mats were shown in Fig. 3. PMMA based fiber mats has T_g value of 130 °C and PMMA-SF fibers did not alter the characteristic T_g of PMMA as shown in Fig. 3. PMMA + PEI nanofiber mats showed a T_g at 17 °C and Tm at 142 °C which was attributed to the presence of PEI. PMMA + SF + PEI nanofiber mats disappeared the T_g at 17 °C and puched the T_m to 169 °C. In addition we recorded an exothermic bump around 127 °C.

3.4. Tensile testing of fiber mats

Next, we investigated the change in mechanical properties, in particular tensile properties of PMMA when combined with SF and PEI. The universal testing machine used to extend the dogbone shape nanofiber mats and the measured elastic modulus values of fibers were given in Table 2. The structural integrity of PMMA nanofiber mats were not as robust as the PMMA + SF, PMMA + PEI or PMMA + SF + PEI nanfiber mats as some of the PMMA test samples broken before the stretching began. Tensile stress recorded for PMMA + SF mats were approximately 25% smaller than PMMA only nanofiber mats. While PMMA + PEI nanofiber mats have 14% higher tensile stress compared to PMMA nanofiber mats. While adding SF or PEI did not significantly altered elastic modulus of PMMA, addition of SF and PEI together resulted in a 52% increase in elastic modulus compared to PMMA only fibers. Tensile stress values of PMMA + SF + PEI nanofiber mats were almost two fold higher than that of PMMA nanofiber mats.

3.5. Antibacterial properties of fiber mats

In order to test the antibacterial activity of resulting fiber mats, we have chosen a *P. aeruginosa* which is rod-shaped gram-negative pathogenic bacterium to be an oral pathogen and further associated with heart and lung infections. The PMMA, PMMA + SF, PMMA + PEI and PMMA + SF + PEI discs were placed on *P. aureginosa* seeded agar plates and incubated overnight. Fig. 4 shows the photographs of agar plates after overnight incubation. The PMMA + PEI and PMMA + SF + PEI mats have shown to inhibit bacterial growth by creating a inhibition zone around the membrane along with a control mat (soluble PEI soaked filter paper).

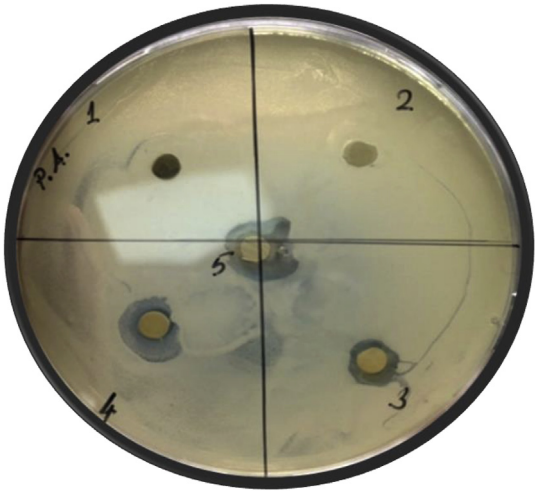

Fig. 4. Antibacterial zone formation around disc shaped PMMA (1), PMMA + SF (2), PMMA + PEI(3), PMMA + SF + PEI(4) and soluble PEI control (5) *P. aeruginosa* seeded agar plate after overnight incubation.

4. Discussion

In this study, we devised a novel strategy to improve antibacterial properties of PMMA without sacrificing on its mechanical properties. Electrospinning PMMA has successfully utilized in earlier studies such as bone tissue engineering [24], mechanotransduction [25] or improving nanoparticle uptake [26]. In addition, PMMA is gold standard material in many dental applications in which studies focusing on improving the mechanical properties of the PMMA based materials received attention [1]. Polyblend electrospinning allowed us to take advantage of combining the properties of all three polymers. It is challenging to produce homogenous polyblend fibers and thus important to consider the dispersity of the polymers that result fibrils otherwise cannot be created with each of the polymers alone. When we combined PMMA, PEI and SF we created nanofiber mats with significantly smaller fiber diameters as shown in Fig. 1D. The almost two fold decrease in fiber diameter in PMMA + PEI + SF nanofiber mats did not appear either of the polymers was combined with PMMA alone. Therefore we concluded that the striking difference in fiber diameters is only observed when both SF and PEI is blended in the PMMA polymer solution before electrospinning. The SEM imaging of fibril morphology after addition of SF particles showed that the particles blended into the fibril topography rather than staying spherical. The homogenous fiber architecture stated that during electrospinning SF microparticles co-spun successfully with PMMA. When combined with PEI and PMMA, SF particles not only cospun with other polymers but also formed charge-charge interactions. The resulting fibers spun into fibrils that are almost half the size of the PMMA fibers that are weight equivalent to the PMMA + SF + PEI fibers. The increased overall surface area due to

Table 2
Elastic properties of PMMA, PMMA-SF, PMMA-PEI and PMMA–SF–PEI fiber mats (n = 4–7) (Results are reported as average ± Standard error).

	PMMA	PMMA + SF	PMMA + PEI	PMMA + SF + PEI
Tensile Stress (N/mm^2)	0,02748 ± 0.008	0,02015 ± 0.0022	0,03112 ± 0.0067	0,06015 ± 0.0061
Elastic Modulus (MPa)	0,03795 ± 0.025	0,02063 ± 0.0018	0,03404 ± 0.0069	0,05804 ± 0.0064

decreased fiber diameter ultimately led to changes observed both in mechanical and thermal properties of the PMMA + SF + PEI mats. In our study we argue that the resulting enhancement in PMMA fibers could potential be a utility for denture resins. For instance, embedding non-woven unidirectional glass fibers in denture resin earlier proven to improve flexural properties [8]. Embedding nonwoven fibers to improve mechanical strength adopted in different resin materials as well. In a 2010 study, Sun et al. processed postdrawn Poly(acrylonitrile) (PAN)-PMMA fibers and created a composite using 2,2-bis-[4-(methacryloxypropoxy)-phenyl]-propane (Bis-GMA) as restorative resin material. They showed the embedded nonwoven fibers increased tensile strength and flexural strength. By choosing the embedding polymer appropriately, this study showed resin material properties can be tailored [18].

SF has been both electrospun alone and cospinned with polymers [27,28]. One of the main drawback for electrospinning SF is the limited number of solvent choices in order to protect tertiary structure of silk fibroin. Hexafluoroisopropanol, formic acid are solvent of choice when processing SF. However harsh, highly polar organic solvents used in electrospinning such as dimethylformamide (DMF), tetrahydrofuran (THF) or dicloromethane (DCM) reported to interfere with the secondary and tertiary structure of silk fibroin [29]. In this study, we preprocessed soluble SF into microparticles and introduced into DMF solution before electrospinning. FTIR results in Fig. 2 showed that the Amide I bonds characteristic in SF FTIR spectra is preserved after electrospinning. Appearance of chemical signatures unique to PEI in PMMA fibrils when both blended before spinning suggests that resulting fibers have both PMMA and PEI chemical information. The PMMA + PEI + SF nanofiber mats thus resulted in formation of free COOH groups and CN bonds suggesting presence of newly formed bonds. Along with changes in fiber diameters and chemical characteristics, PMMA + PEI + SF fibers also showed drastic changes in thermal properties. PMMA has a Tg value of 130 °C in the literature while PEI is a hyperbranched low molecular weight polymer. The literature suggests the linear PEI has a melting point of 59–64 depending on the molecular weight. PMMA + PEI mats show a transition at 25 °C owing to PEI and 120 °C owing to PMMA, the melting temperature of PEI resulted after the PMMA in mats past its T_g. However, adding SF alone in PMMA + SF nanofibers did not change the T_g of PMMA suggesting the SF may not be homogenously incorporated into the fibrils. The thermal behavior of PMMA + PEI + SF fibers further increased melting of PEI in the mats since SF has a T_m of 180 °C suggesting incorporated SF modulate thermal properties of the PMMA + PEI + SF nanofiber mats [30].

In our study we tested addition of 1% w/vol SF into PMMA fibers. The change in tensile strength was not significant compared to PMMA, however when PMMA + SF + PEI is combined, both the tensile strength and the elastic modulus of the fibers increased significantly. We argue that not only the addition of SF but also PEI resulted in decreased fibril diameter. The fibril diameter with decreased overall porosity could effectively increase the tensile strength. While this is owing to presence of both SF and PEI, we concluded that both polymers are necessary in our materials design. While SF received appreciation in tissue engineering field, not many studies focused on its applicability in dental restoration materials. In 2015, Rameshbabu et al. added alumina, SF short fibers in Bis-GMA resin materials to improve mechanical properties. While SF have shown to improve elastic strength, it is not yet defined clearly what is the minimum percentage of SF to be effective in the resulting material.

Our strategy allowed sustaining PEI within the polymer matrix while maintaining its antibacterial activity. Both the PMMA + PEI and PMMA + SF + PEI fiber mats exhibited antibacterial activity against *P. aureginosa* indicating the antibacterial activity of mats is originated from PEI. Shvero et al. embedded PEI based nanoparticles (NP) into polymer resin before the polymerization process was initiated and showed 1% w/w was enough to prevent growth of oral pathogens such as *S. mutans, L. caseii, A. viscosus, E. fecalis* and even whole saliva isolates suggesting wide range of protection within the oral flora [31]. PEI based NPs effect on bacterial formation persisted on both outer and inner surface of the resin material, however their x-ray photoelectron spectroscopy (XPS) measurements indicated the particles distributed unevenly aggregating mostly at the inner regions. Another study by Pietrokovsky used quaternary ammonium PEI (QPEI) NPs and reported that 1% QPEI to prevent growth of *S. mutans* and *A. viscosus* two oral pathogens found on the dental caries and the surface of dental implants [10]. Both studies reported that embedded PEI NPs interfere with the resin during polymerization and change the degree of conversion and did not further investigated the effect of added PEI NPs on mechanical properties of resins. PEI also used in its unmodified form to generate colloidal stability for silver nanoparticles and successfully shown to increase silver NP size without compromising on the antibacterial effects and decreased cytotoxicity which is the main problem with silver nanoparticles [32]. The resulting fibers are intrinsically antibacterial against *P. aeuroginosa* and mechanically superior to PMMA alone. Ultimately, the produced nanofiber mats have potential towards applications in PMMA based denture resins towards overcoming the drawbacks of current PMMA resins.

5. Conclusion

In this study, we utilized electrospinning as a strategy towards combining PMMA, PEI and SF to build an intrinsically antibacterial and mechanically superior new material. We have combined PMMA with SF microparticles and hyperbranched low molecular weight PEI and electrospun into small fibrils. The resulting material showed increased elastic modulus and tensile stress compared to PMMA only fibrils. Additionally thermal properties also altered when PMMA, SF and PEI combined into fibrils leading to higher melting temperatures. The antibacterial activity of resulting fibers tested against *P. aeuroginosa* and found the both PMMA + PEI and PMMA + PEI + SF fibers showed antibacterial activity possibly due to highly cationic PEI component. This new material holds potential towards improvement of denture based materials.

Declaration of competing interest

None.

Acknowledgements

Authors would like to thank Prof. Cemil Alkan, Prof. Eyyup Gercekcioglu and Prof. Isa Gokce for their valuable support in sharing their laboratory equipment during the course of this study. Dr Ali Ozer for his expert assistance in SEM imaging. Authors would also thank Prof. Justin L. Brown for sharing valuable comments and revision of the manuscript. This work was supported in part by Turkish Science and Technology Agency (TUBITAK, 3001 program, 217M910) (to T.O.).

Appendix A. Supplementary data

Supplementary data to this article can be found online at https://doi.org/10.1016/j.bioactmat.2020.04.005.

References

[1] R. Bhola, et al., Biocompatible denture polymers-a review, Trends Biomater. Artif. Organs 23 (3) (2010) 129–136.
[2] E. Battistella, et al., Degradable polymers may improve dental practice, J. Appl. Biomater. Biomech. 9 (3) (2011) 223–231.
[3] R. Goseki, T. Ishizone, Poly(methyl methacrylate) (PMMA), in: S. Kobayashi, K. Müllen (Eds.), Encyclopedia of Polymeric Nanomaterials, Springer Berlin Heidelberg, Berlin, Heidelberg, 2021, pp. 1–11.
[4] S.D. Heintze, D. Monreal, V. Rousson, Fatigue resistance of denture teeth, J. Mech. Behav. Biomed. Mater. 53 (2016) 373–383.

[5] S. An, Influence of the Addition of Microencapsulated Phytoncide to a Denture Base Resin on Mechanical Properties and Antimicrobial Activity, (2017).
[6] N.W. Elshereksi, et al., Perspectives for titanium-derived fillers usage on denture base composite construction: a review article, Adv. Mater. Sci. Eng. (2014) 1687–8434 https://doi.org/10.1155/2014/746252.
[7] M. Vojdani, R. Giti, Polyamide as a denture base material: a literature review, J. Dent. 16 (1 Suppl) (2015) 1.
[8] M.M. Gad, et al., PMMA denture base material enhancement: a review of fiber, filler, and nanofiller addition, Int. J. Nanomed. 12 (2017) 3801–3812.
[9] M. Su, et al., Antibacterial effect and bond strength of a modified dental adhesive containing the peptide nisin, Peptides 99 (2018) 189–194.
[10] Y. Pietrokovski, et al., Antibacterial effect of composite resin foundation material incorporating quaternary ammonium polyethyleneimine nanoparticles, J. Prosthet. Dent 116 (4) (2016) 603–609.
[11] N. Beyth, et al., Surface antimicrobial activity and biocompatibility of incorporated polyethylenimine nanoparticles, Biomaterials 29 (31) (2008) 4157–4163.
[12] J.G. Hardy, L.M. Römer, T.R. Scheibel, Polymeric materials based on silk proteins, Polymer 49 (20) (2008) 4309–4327.
[13] D. Ebrahimi, et al., Silk-its mysteries, how it is made, and how it is used, ACS Biomater. Sci. Eng. 1 (10) (2015) 864–876.
[14] X. Zhang, M.R. Reagan, D.L. Kaplan, Electrospun silk biomaterial scaffolds for regenerative medicine, Adv. Drug Deliv. Rev. 61 (12) (2009) 988–1006.
[15] M. Stoppato, et al., Effects of silk fibroin fiber incorporation on mechanical properties, endothelial cell colonization and vascularization of PDLLA scaffolds, Biomaterials 34 (19) (2013) 4573–4581.
[16] R. Murugan, et al., Nanofibrous scaffold engineering using electrospinning, J. Nanosci. Nanotechnol. 7 (12) (2007) 4595–4603.
[17] Anitha Ravikrishnan, et al., Regulation of Epithelial-to-Mesenchymal Transition Using Biomimetic Fibrous Scaffolds, ACS Appl. Mater. Interfaces 8 (28) (2016) 17915–17926.
[18] W. Sun, et al., Post-draw PAN-PMMA nanofiber reinforced and toughened Bis-GMA dental restorative composite, Dent. Mater. 26 (9) (2010) 873–880.
[19] S. Wang, et al., Colloidal stability of silk fibroin nanoparticles coated with cationic polymer for effective drug delivery, ACS Appl. Mater. Interfaces 7 (38) (2015) 21254–21262.
[20] S.F. Curling, C.A. Clausen, J.E. Winandy, Relationships between mechanical properties, weight loss, and chemical composition of wood during incipient brownrot decay, For. Prod. J. 52 (7/8) (2002) 34–39.
[21] P. Kalakonda, S. Banne, Thermomechanical properties of PMMA and modified SWCNT composites, Nanotechnol. Sci. Appl. 10 (2017) 45–52.
[22] R. Xu, et al., Preparing sodium alginate/polyethyleneimine spheres for potential application of killing tumor cells by reducing the concentration of copper ions in the lesions of colon cancer, Materials 12 (9) (2019).
[23] H. Zhang, et al., Preparation and characterization of silk fibroin as a biomaterial with potential for drug delivery, J. Transl. Med. 10 (2012) 117.
[24] T. Ozdemir, et al., Substrate curvature sensing through Myosin IIa upregulates early osteogenesis, Integr. Biol. (Camb) 5 (11) (2013) 1407–1416.
[25] T. Ozdemir, et al., Identification of key signaling pathways orchestrating substrate topography directed osteogenic differentiation through high-throughput siRNA screening, Sci. Rep. 9 (1) (2019) 1001.
[26] C. Huang, et al., The role of substrate topography on the cellular uptake of nanoparticles, J. Biomed. Mater. Res. B Appl. Biomater. 104 (3) (2016) 488–495.
[27] Y. Gao, et al., Biomineralized poly (l-lactic-co-glycolic acid)-tussah silk fibroin nanofiber fabric with hierarchical architecture as a scaffold for bone tissue engineering, Mater. Sci. Eng. C 84 (2018) 195–207.
[28] J. Zhu, et al., Electrospun homogeneous silk fibroin/poly (varepsilon-caprolactone) nanofibrous scaffolds by addition of acetic acid for tissue engineering, J. Biomater. Appl. 31 (3) (2016) 421–437.
[29] L. Jeong, K.Y. Lee, W.H. Park, Effect of solvent on the characteristics of electrospun regenerated silk fibroin nanofibers, Key Engineering Materials, Trans Tech Publ, 2007.
[30] D.T. Pham, N. Saelim, W. Tiyaboonchai, Crosslinked fibroin nanoparticles using EDC or PEI for drug delivery: physicochemical properties, crystallinity and structure, J. Mater. Sci. 53 (20) (2018) 14087–14103.
[31] D.K. Shvero, et al., Characterisation of the antibacterial effect of polyethyleneimine nanoparticles in relation to particle distribution in resin composite, J. Dent. 43 (2) (2015) 287–294.
[32] H.J. Lee, et al., Antimicrobial polyethyleneimine-silver nanoparticles in a stable colloidal dispersion, Colloids Surf. B Biointerfaces 88 (1) (2011) 505–511.